TERM

ORIGINAL ARTICLE

Near-infrared Transillumination and Photodynamic Therapy Using Hypericin in Animal Laryngeal Tumors

Haeyoung Lee[1] · Sung Won Kim[2,3] · Daa Young Kwon[3,4] · Hyun Wook Kang[4] · Min-Jung Jung[5] · Jun Hyeong Kim[6] · Yeh-Chan Ahn[3,4] ⓘ · Chulho Oak[3,6]

Abstract

BACKGROUND: We aimed to validate a pilot study of photodiagnosis using near infrared (NIR) transillumination and assess the clinical efficacy of hypericin-mediated photodynamic therapy (HYP-PDT) in a rabbit laryngeal cancer model in order to develop a novel therapeutic modality with complete remission and preservation of the functional organ.

METHODS: (1) *In vitro* study: VX tumor cells were subcultured and subjected to HYP-PDT. (2) *In vivo* study: A laryngeal cancer model was developed in which 12 rabbits were inoculated with a VX tumor suspension in the submucosal area of the left vocal fold using a transoral approach. All rabbits underwent NIR transillumination using light with a wavelength of 780 nm. The survival periods of the three treatment groups (6 rabbits in Group A: HYP-PDT, 3 each in Groups B and C: laser irradiation or HYP administration only) were analyzed.

RESULTS: The higher the HYP concentration, the lower the VX cell viability in response to HYP-PDT using 590 nm LED. Following HYP-PDT, small tumors in Group A-1 rabbits healed completely and the animals demonstrated a long survival period, and larger tumors in Group A-2 healed partially with a survival period that extended over 3 weeks after inoculation. The survival of Groups B and C were not different over the first 3 weeks of the study, and were shorter than in Group A.

CONCLUSION: We found HYP-PDT could be a curative therapy for early-stage cancers that may also preserve organ function, and may inhibit tumor progression and metastasis during advanced stages of laryngeal cancer.

Keywords Hypericin · Photodynamic therapy · Laryngeal cancer

Haeyoung Lee, Sung Won Kim and DaaYoung Kwon have contributed equally to this work.

✉ Yeh-Chan Ahn
ahny@pknu.ac.kr

✉ Chulho Oak
oaks70@daum.net

1 Department of Thoracic and Cardiovascular Surgery, Kosin University College of Medicine, Busan 49267, Korea

2 Department of Head and Neck Surgery and Otolaryngology, Kosin University College of Medicine, Busan 49267, Korea

3 Kosin Innovative Smart Healthcare Research Center, Kosin University Gospel Hospital, Busan 49267, Korea

4 Department of Biomedical Engineering and Center for Marine-Integrated Biomedical Technology, Pukyong National University, Busan 48513, Korea

5 Department of Pathology, Kosin University College of Medicine, Busan 49267, Korea

6 Department of Internal Medicine, Kosin University College of Medicine, Busan 49267, Korea

1 Introduction

Squamous cell carcinoma (SCC) of the larynx is one of the most common cancers and is associated with a poor prognosis [1]. Initial diagnosis of early-stage cancer, and preservation of organ function and capacity for tissue regeneration in locally advanced stages of cancer are all critical factors with respect to life expectancy and life quality [2–4]. Therefore, laser surgery has become the standard treatment option for SCC of the larynx [2]. Recent technological developments are also providing additional non-invasive imaging modalities to visualize the larynx, including optical coherent tomography and ultrasound, among others. [5, 6].

Near-infrared light transillumination (NIRT) was introduced into clinical settings [7, 8]. Rather than using cold visible light, NIR-transillumination was modified to use invisible, near-infrared light of longer wavelengths [9]. This process reduces light scattering effects and allows deeper light penetration into bony tissue [7, 8]. Despite the benefits of NIR with regard to tissue penetration, NIR transillumination of the vocal cord including tumor is potentially challenging. In this study, we report the first investigation of transillumination to detect laryngeal tumors.

With regard to organ-preserving therapeutic modalities, photodynamic therapy has been one of preferred treatment options because of its selective tumoricidal effects with preservation of normal tissue [10]. In the 2000s, the photosensitizer hypericin (HYP) was first used for tumor localization owing to selective accumulation in tumor tissues and lack of toxicity [11]. After a specific incubation period, the photosensitizer-illuminated tumor can be observed under visible light, which, in the presence of oxygen, activates processes that exert cytotoxic effects, such as cell apoptosis and necrosis.

Various cell lines have been used for *In vitro* HYP-mediated PDT (HYP-PDT) experiments [12–14]. One study demonstrated that various signaling pathways are activated upon the administration of HYP-PDT. The cellular toxicity differs at the molecular level depending on the amount of irradiated light. A high dose of light induces cell necrosis, while a medium dose induces alterations in the activities of key mediators, such as caspase, cytochrome C, and mitochondrial calcium ions, resulting in the initiation of apoptosis via a different pathway. A low dose of light triggers the MAPK pathway (mitogen-activated protein kinase pathway) resulting in cell survival and angiogenesis [15]. Moreover, HYP exhibits anti-metastatic activity in the absence of light, and inhibits migration and invasion of endothelial cells, as evidenced by the approximately two-fold greater survival rate of mice with HYP accumulation in the lungs compared to that of control mice. Following treatment with hypericin, long-term survival increased to 34.5% compared with 15.6% in controls and 46.1% compared with 17.7% in controls in murine breast adenocarcinoma (DA3) and squamous cell carcinoma (SQ2) models, respectively.

2 Materials and methods

2.1 Induction of carcinoma in rabbits and VX tumor cells

Carcinoma was induced in a New Zealand white rabbit (Taesung Laboratory Animal Science, Busan, Korea) model. A modified version of the tumor model described by Ahn et al. was used in this study [5].

Briefly, following sectioning of the tumor tissue, the tumor cell suspension was treated with collagenase (Gibco®, Thermo Fisher Scientific Korea Ltd., Seoul, Korea) for 30 min. The cells were cultured in Dulbecco's Modified Eagle's Medium/Nutrient Mixture F-12 Ham (DMEM/F-12, Corning) containing 15 mM HEPES (4-(2-hydroxy ethyl)-1-piperazine ethane sulfonic acid), 20% fetal bovine serum (FBS; Hyclone®, GE Healthcare Life Sciences Korea Ltd., Seoul, Korea) and 1X antibiotic–antimycotic solution (Gibco®, Thermo Fisher Scientific Korea Ltd.) in a 60-mm culture plate and incubated at 37 °C in an incubator containing 5% CO_2 and 95% humidity. After 2 to 3 weeks, cells from colonies were isolated using TrypLE™ (Gibco, Thermo Fisher Scientific Korea Ltd.) and successively subcultured and transfer to new culture plates. These tumor cells developed into fibroblast-shaped cancer cells, named VX tumor cells.

To examine HYP cytotoxicity in VX tumor cells, the cells were re-cultured for 24 h. During the reculturing, 10^4 VX tumor cells per well were added to 96-well plates and the plates incubated for 24 h, and the cells were then treated with 10, 3, 1 or 0.3 μM of HYP. The cell viability was evaluated by measuring the absorbance at 450 nm.

2.2 *In vitro* HYP-PDT

The VX tumor cells were cultured in 96-well plates at 10^4 cells per well in DMEM/F-12 (Corning) containing 100 μL of 15 mM HEPES, 20% FBS (Hyclone®, GE Healthcare Life Sciences Korea Ltd.) and 1 X antibiotic–antimycotic (Gibco, Thermo Fisher Scientific Korea Ltd.) in a culture plate 60 mm in diameter and incubated for 24 h at 37 °C in an incubator containing 5% CO_2 and 95% humidity. Subsequently, the VX tumor cells were washed twice with PBS and irradiated with a 590 nm LED light source (M590, Thorlabs, Newton, NJ, USA) for 30 min.

In order to evaluate VX tumor cell variability, the cells were cultured for an additional 24 h after irradiation and the absorbance was measured at 450 nm using a VICTOR3 Multilabel Counter 1420 (PerkinElmer Korea, Seoul, Korea) after an incubation period of 2 h using a Cell Counting Kit-8 (CCK-8, Dojindo Molecular Technologies, Inc., Rockville, MD, USA) reagent. To evaluate apoptotic effects mediated by intracellular caspases, the cells were treated with 20 µM of Z-VAD-FMK (R&D Systems Inc., Minneapolis, MN, USA), which is a pan-caspase inhibitor. The tumor cell viability was measured and compared between treatment and non-treatment groups. All experiments were performed in triplicate [16].

2.3 VX tumor cell preparation and injection into the submucosal layer of the left vocal cord in the larynx

We conducted all animal procedures in accordance with the guidelines published by the Guide for the Care and Use of Laboratory Animals (DHEW publication NIH 85–23, revised 2010, Office of Science and Health Reports, DRR/NIH, Bethesda, MD, USA). The protocol of this experiment was approved by the Committee of Animal Research. We used 12 male New Zealand white rabbits (Taesung Laboratory Animal Science, Busan, Korea) weighing 3.0 to 3.7 kg, housed in separate cages at a controlled temperatures of 22 ± 2 °C with $55 \pm 5\%$ humidity [17].

The preparation and inoculation of VX tumor cells was as described in the study of Ahn et al. Briefly, we administered general anesthesia comprising 35 mg/kg ketamine and 5 mg/kg xylazine intramuscularly. Each rabbit was placed in the supine position on the operating table with the body temperature maintained at 39 °C while monitoring the rectal temperature, heartbeat, and respiratory rate. After extension of the neck, the mouth was opened and the tongue pulled out, and the larynx was observed using a rigid laryngoscope (Karl Stortz, GmbH & Co. KG, Tuttlingen, Germany) and video monitoring system. The VX tumor cell suspension was loaded into a 1-cc syringe with a 26-gauge needle attached and was injected into the submucosal area of the left vocal fold using a transoral approach (Fig. 1).

The 12 rabbits were divided into 3 groups. Figure 2 shows the schematic diagram of the *in vivo* study. Group A (experimental group) included 6 rabbits that were subjected to HYP-PDT. Group B consisted of 3 rabbits that were only subjected to laser irradiation. Group C consisted of 3 rabbits that were administered HYP only. Hence, 2 control groups were included. Based on the tumor size and extension to the midline of the vocal cord, Group A was subdivided into Group A-1 comprising animals with small tumors that did not cross the midline and Group A-2 comprising animals with larger tumors crossing the midline.

2.4 *In vivo* validation of near-infrared transillumination of laryngeal tumors

The NIR-transillumination system was composed of two parts. The first part, the transoral approach, consisted of a USB CMOS camera board with its infrared filter removed, inserted into a custom 3D-printed wand housing. The second part, the trans-cricothyroidal approach, consisted of a 780-nm LED used as the illumination source (Fig. 3). Laryngeal tumors were examined during the early (1 week after tumor inoculation) and advanced (2 weeks after tumor inoculation) stages of laryngeal cancer using a transoral endoscope with the rabbits placed in a supine position. With the lights of the transoral endoscope off, transoral endoscopy with a near-infrared (NIR) light source was used to illuminate the larynx in the subglottic to supraglottic direction. The tumor delineation was confirmed by NIR transillumination. Finally, the tumor imaging results were verified by comparing them with the tumor morphology and depth of invasion obtained from a pathology examination.

2.5 Photodynamic diagnosis, therapy, and evaluation of the therapeutic effects

One week following the injection of the VX tumor cell suspension, photodynamic diagnosis (PDD) using HYP was performed when the tumor could be detected with rigid laryngoscopy.

After intravenous injection of 5 mg/kg of HYP into the marginal ear vein using a 3-cc syringe with 26-gauge needle attached, selective accumulation of HYP in the tumor tissue was detected using a rigid laryngoscope with a transoral plastic tube porter with a 5 mm inner diameter; the rabbits were in the supine position under general anesthesia, similar to the positioning during tumor cell inoculation. We observed laryngeal cancers with white light (WL) and autofluorescence (AF) mode using the D-Light AF light source (Karl Stortz). In AF mode, an emission filter (MF630-69, Thorlabs) with a 630 nm bandpass with 69 nm FWHM was inserted between the rigid laryngoscope and camera head (Karl Stortz Image 1 HD H3-Z) to filter extraneous wavelengths, while admitting the fluorescence wavelength emitted from the HYP accumulated in the tumor.

After PDD, we treated Groups A and B with 500 mW and 500 J (Ceralas PDT Laser System) of laser irradiation using an optical diffusing fiber (core diameter = 600 µm; TeCure, Busan, Korea), positioned at the level of the vocal cord in the same position. The micro-machined surface of
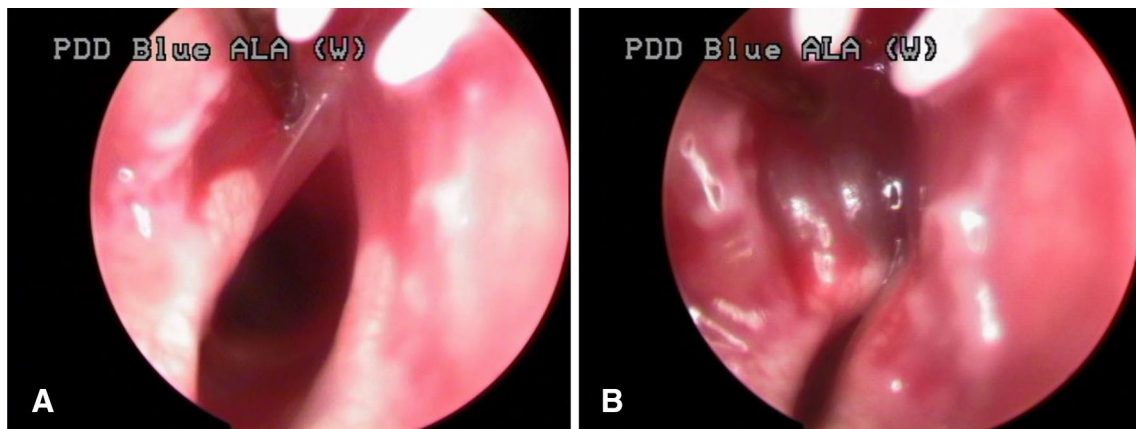
Fig. 1 Video-assisted transoral endoscopic injection of VX tumor cells into the submucosal area of the left vocal cord. **A** A tip of needle was inserted into left vocal cord. **B** Mucosal swelling after injection of tumor cells
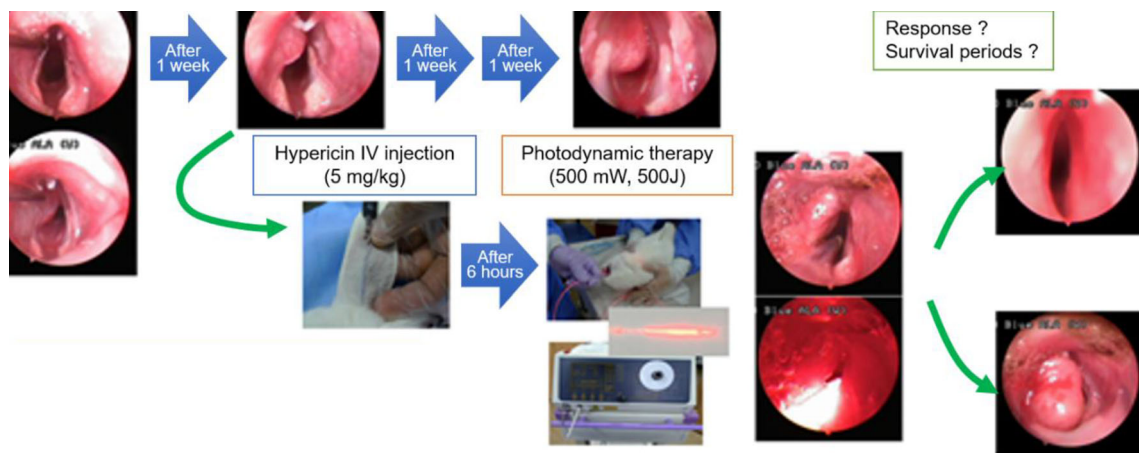

Fig. 2 Schematic representation of the *in vivo* experimental procedures. A total of 12 rabbits were divided into 3 groups. Group A (experimental group) included 6 rabbits subjected to HYP-PDT, while another 3 rabbits were assigned to Group B that received laser treatment only, and the other 3 rabbits were assigned to Group C treated with HYP only (i.e., 2 control groups). Group A was subdivided according to tumor size and extension to the midline of the vocal cord, with Group A-1 representing rabbits with tumors of smaller size that did not cross the midline and Group A-2 representing rabbits with larger tumors that crossed the midline
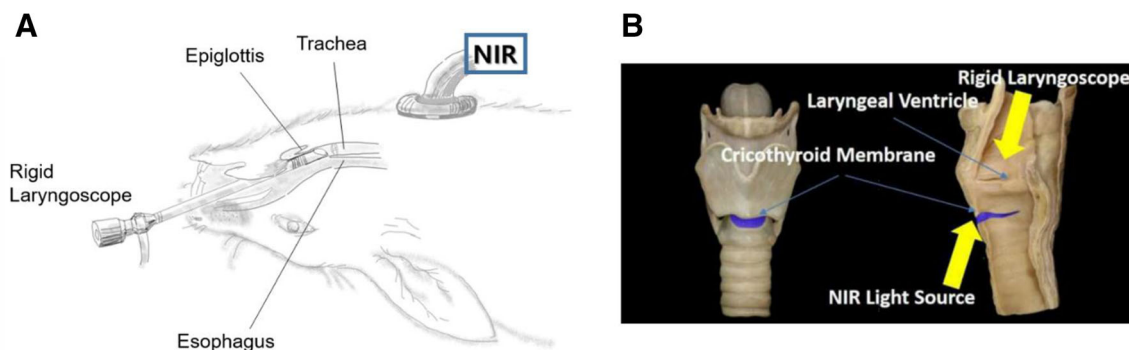

Fig. 3 *In vivo* images of the left vocal cord were acquired with a rigid laryngoscope using the laryngoscope and NIR as the light source. **A** Gross depiction. The tumor was observed on the left membranous vocal fold. **B** Anatomical depiction. The tumor delineation was confirmed by NIR transillumination

the fiber emitted the incident laser energy circumferentially to the tissue surface with a deviation of less than 0.1 (i.e., normalized intensity = 0.9 ± 0.1). Group C was treated only with intravenous HYP without laser irradiation. We

assessed the change in the shape of laryngeal cancer, the mechanism by which the airway space was narrowed, and the development of asphyxia at weekly intervals.

3 Results

3.1 Evaluation of cytotoxicity in VX tumor cells based on HYP concentration

The VX tumor cells were re-cultured for 24 h. The cells were cultured at 10^4 cells per well in 96-well plates, incubated for 24 h, and then treated with 10, 3, 1, or 0.3 μM of HYP. Subsequently, the cell viability was measured. The cytotoxic effects were insignificant at concentrations lower than 3 μM, but higher HYP concentrations produced high cytotoxicity in VX tumor cells,

The VX tumor cells were treated with HYP for 1 h in the culture medium without serum, and then irradiated with a 590-nm LED after the addition of culture medium containing serum. Subsequently, VX tumor cells were cultured in a light-shielding incubator for 24 h and the cell viability was measured. Viability in tumor cells subjected to HYP-PDT with 590 nm LED was reduced in an HYP-concentration-dependent manner.

3.2 Verification of caspase activation

In order to demonstrate that the loss of viability was primarily related to caspase activation of the apoptosis pathway induced by HYP-PDT treatment followed by irradiation with a 590 nm LED, we incubated the VS cells with Z-VAD-FMK, a pan-caspase inhibitor. The cell viability improved owing to the inhibition of the apoptosis pathway by HYP-PDT (Fig. 4).

3.3 Development of laryngeal tumor model and NIR transillumination

Figure 5 shows representative endoscopic images of laryngeal cancer in the rabbit model obtained on Days 3, 6, 9 and 12 after tumor inoculation (Fig. 6).

In the transillumination images, the normal larynx appeared smooth and homogenous in texture because there was no characteristic bony structure while reduced translucency throughout tumor is indicative of areas of overall tumor margin. Videoendoscopic images of the laryngeal tumors demonstrated the submucosal tumor protruding from the mucosal surface, which prevented assessment of the tumor margins that were obscured by the tumor invasion. However, when using the NIR system to scan along the margins of the protrusion, a tumor margin
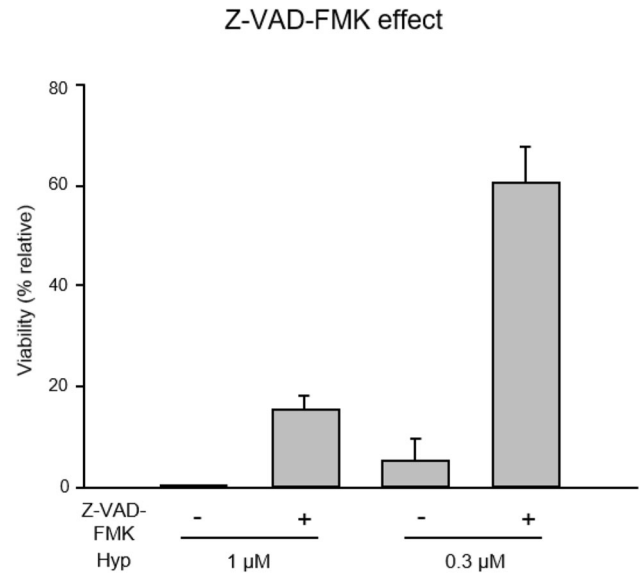

Fig. 4 Effect of Z-VAD-FMK on apoptosis induced by hypericin-mediated photodynamic therapy. Apoptosis induced by caspase activation due to hypericin-mediated photodynamic therapy together with 590 nm LED was inhibited by the pan-caspase inhibitor, Z-VAD-FMK. The Z-VAD-FMK improved the survival rate by inhibiting the apoptosis pathway induced by hypericin-mediated photodynamic therapy

was revealed that was not readily apparent under white light (Fig. 7).

3.4 Endoscopic observations of larynx after photodynamic diagnosis and treatment

One week after tumor inoculation, the tumor developed to produce a protrusion on the left side of the vocal cord and was diagnosed by PDD with WL as the source in Groups A and C was treated with HYP. In AF mode, the larynx exhibited a red color and the protruding portion of the tumor appeared dark red compared to the surrounding normal mucosa. Hence, we were able to assess the margin of the tumor within the surrounding healthy tissue based on the intensity/depth of the red color.

In HYP-untreated Group B, we detected the protruding tumors similar to those seen in the other groups in WL mode, but could not differentiate the tumor from normal mucosa owing to the blue-colored appearance in the AF mode. There was no gross change in the tumor during the initial one-week period after PDT. However, one week post PDT, the tumor mass decreased with peri-tumoral mucosal edema. Two weeks post PDT, superficial necrosis was identified in the tumor tissue, and at 3 weeks post PDT, the tumors and vocal cord edema were eliminated in the two Group A-1 animals that initially had small tumors that did not cross the midline of the vocal cords (Fig. 8).
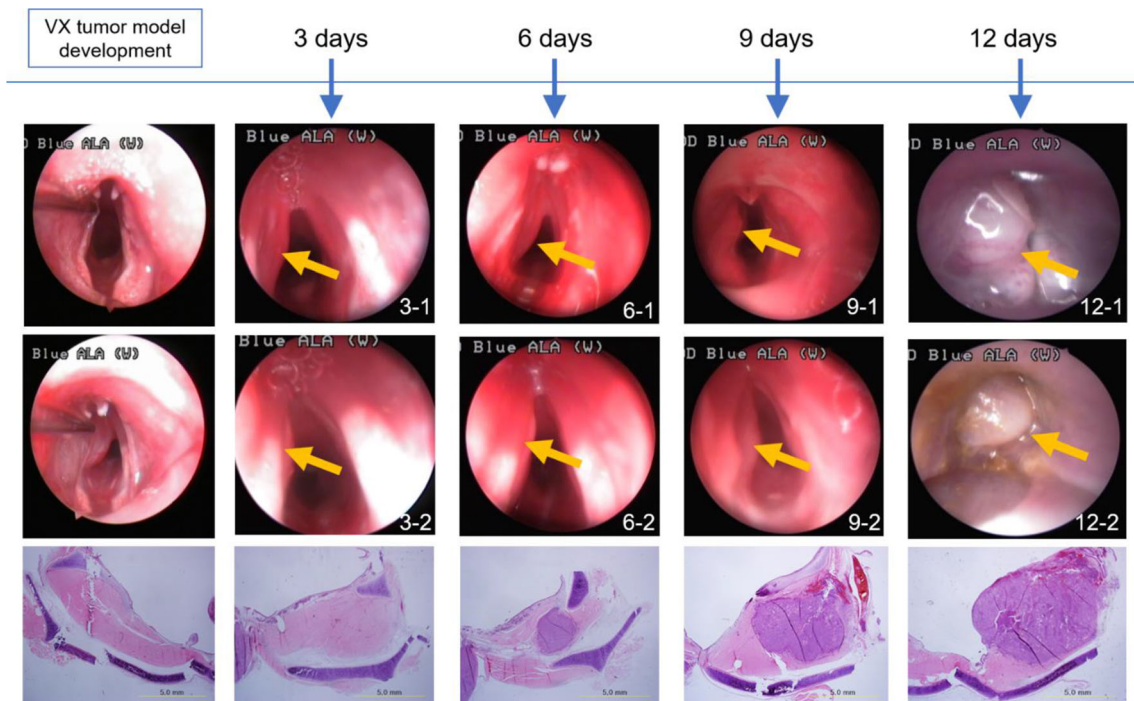
Fig. 5 Endoscopic images were acquired at the indicated number of days (3, 6, 9, and 12) after tumor inoculation in the animal model of vocal cord tumor. The arrow indicates the bulging portion of the tumor. Pathologic images for each were also obtained to confirm the findings
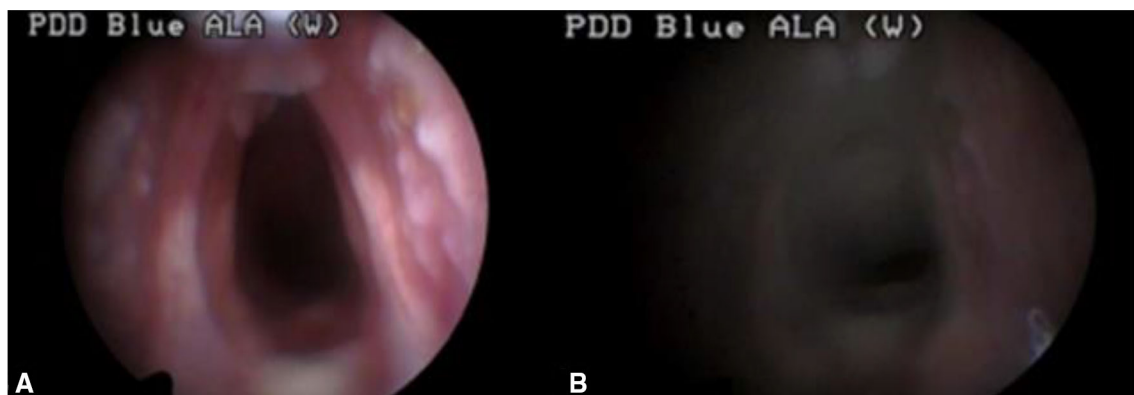

Fig. 6 *In vivo* images of the normal vocal cord acquired with a rigid laryngoscope using **A** the laryngoscope and **B** NIR as the light source
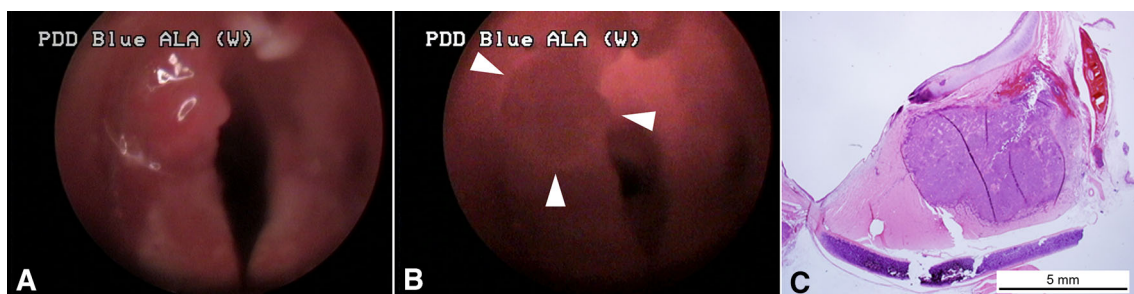

Fig. 7 *In vivo* images of the left vocal cord acquired with a rigid laryngoscope using **A** the laryngoscope and **B** NIR as the light source. The tumor was observed on the left membranous vocal fold (**A**). The tumor delineation (arrow heads) was confirmed by NIR transillumination (**B**). **C** Pathological examination indicative of a localized tumor of left vocal cord. The tumor was localized with vocalis muscle with clear margination (stain, hematoxylin and eosin; magnification, × 10)

Although four animals assigned to Group A-2 with large tumors that crossed the midline showed initiation of superficial mucosal necrosis and survived over 2 weeks, they died 3 to 5 weeks after PDT owing to airway obstruction (Fig. 9).

In the Group B control animals not treated with HYP and subjected to laser irradiation only, no changes in the normal mucosa or the tumor were evident during the study period. All animals died 1 to 2 weeks following the treatment (Fig. 10).

In Group C HYP-only control animals, tumor growth continued and all animals died 1 to 2 weeks after the procedure (Fig. 11).

Selective accumulation of HYP was obtained after 1 week of laser therapy, photodynamic therapy, and hypericin-treated only, respectively, which shows the case in Figs. 10, 8, and 11. (Fig. 12).

The results of the survival curve analysis demonstrated that Group A animals, all of which survived in this study, exhibited a clinically cured status for more than two-fold longer than those of the other groups. There were no differences between groups B and C with respect to tumor progression and natural death (Fig. 13). The comparative overall survival of Groups A and B was 4.5 ± 2.4 week, 2.2 ± 1.5 week ($p = 0.03$), respectively, and Groups A and C, 4.5 ± 2.4 week, 2.3 ± 1.7 week ($p = 0.04$), respectively.

4 Discussion

Laryngeal cancer is one of the most common types of squamous cell carcinoma with respect to clinical incidence rates. Treatment of primary and, in particular, recurrent laryngeal cancer requires alternative therapeutic modalities in order to preserve the functionality of the organ, which is required for phonation [2]. In 1990, Raab et al. [18] introduced the photodynamic reaction as the basic principle of PDT and suggested PDT could serve as a novel, minimally invasive cancer treatment. Since its introduction, PDT has been used to treat cancers in various organs, such as the lung, esophagus, stomach, uterine cervix, and urinary bladder [19]. However, there have been few published reports examining its effects on laryngeal cancer [20–22]. To date, no study examining the effects of HYP-PDT in the orthotopic animal model *in vivo* has been published.

In this study, tumors developed approximately 1 week after tumor inoculation, and were confirmed by rigid laryngoscopy in our experiments [5]. We demonstrated the margins of the laryngeal tumors by NIR transillumination even though the tumors were submucosal in location and had invaded the submucosal layer without clear margins. This was the first study to visualize the overall margins of submucosal laryngeal tumors. In clinical settings, surgeons have reported having great difficulty achieving complete resection of laryngeal tumors because they were unable to visualize the overall tumor margin and depth of invasion [1]. Therefore, we proposed further study of the feasibility
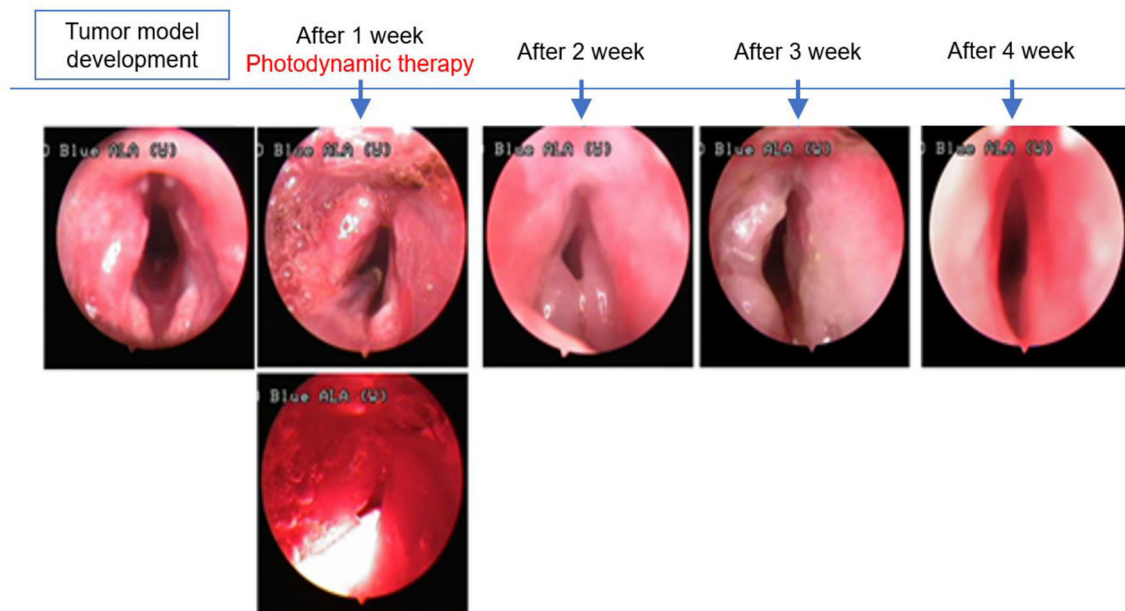

Fig. 8 No gross changes, such as photothermal injury, were observed after photodynamic therapy during the initial period. A week after photothermal therapy, tumor mass decreased with peri-tumoral mucosal edema. Two weeks after PDT, superficial necrosis was observed in the tumor. Small-sized tumors in two animals in Group A-1 that did not cross the midline of the vocal cord healed completely with restoration of vocal cord edema 3 weeks post PDT
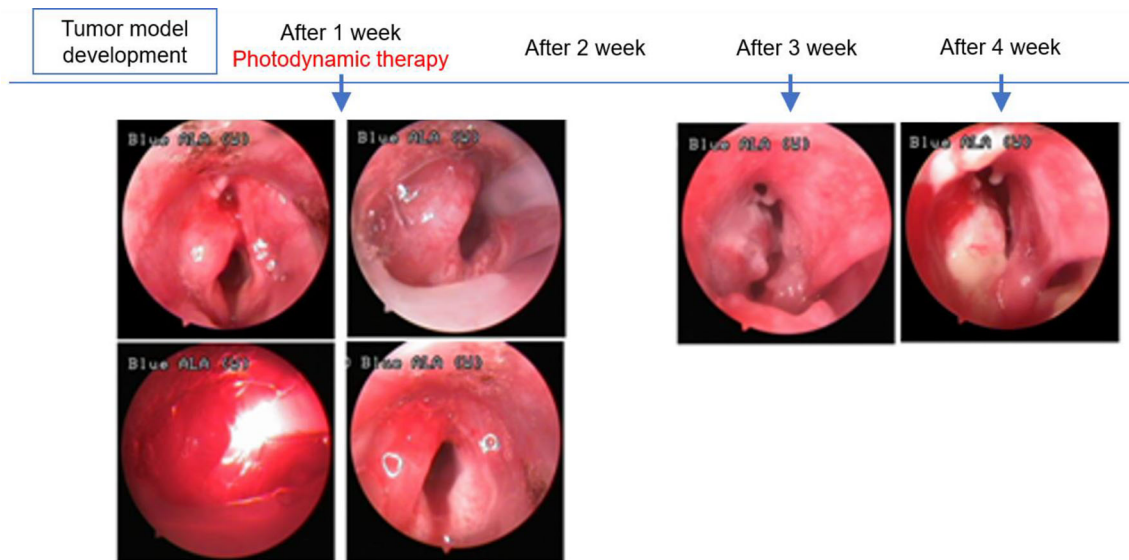
Fig. 9 Four cases of large-sized tumors in Group A-2 that crossed the midline also showed initiation of superficial mucosal necrosis, and the rabbits died 3 to 5 weeks following hypericin-mediated photodynamic therapy owing to airway obstruction caused by regrowth of the cancer tissue
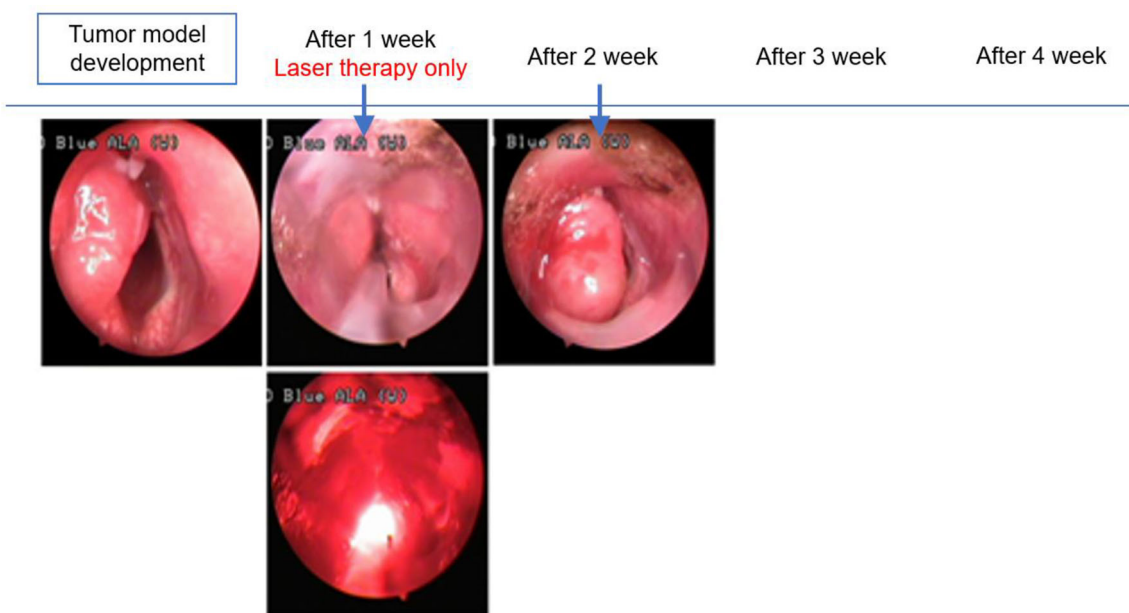

Fig. 10 In Group B rabbits subjected to laser irradiation only (no hypericin) there was no change in the normal mucosa, and tumor growth occurred during the treatment interval. All animals died 1 to 2 weeks after the treatment

of NIR transillumination to visualize the margins of sub-mucosal tumors was warranted. In this study, the animals died when the laryngeal tumor crossed the midline of the vocal cord, resulting in airway obstruction within 3 weeks after inoculation. Therefore, instead of complex calculations to determine the width or volume of airway lumen after computerized tomography or other radiological examinations, the difference in the survival period of the animals was the simplest and most crucial parameter to determine whether HYP-PDT is effective in tumor therapy. We demonstrated that our development of a novel laryngeal cancer model in rabbits and the application of HYP-PDT for its treatment were relatively easy and highly reproducible. We observed complete remission in Group A-1: in contrast to the control groups, the animals belonging to this group survived after tumor inoculation until the end of the 8-week study period and no abnormalities, such as tumor-like characteristics, were detected
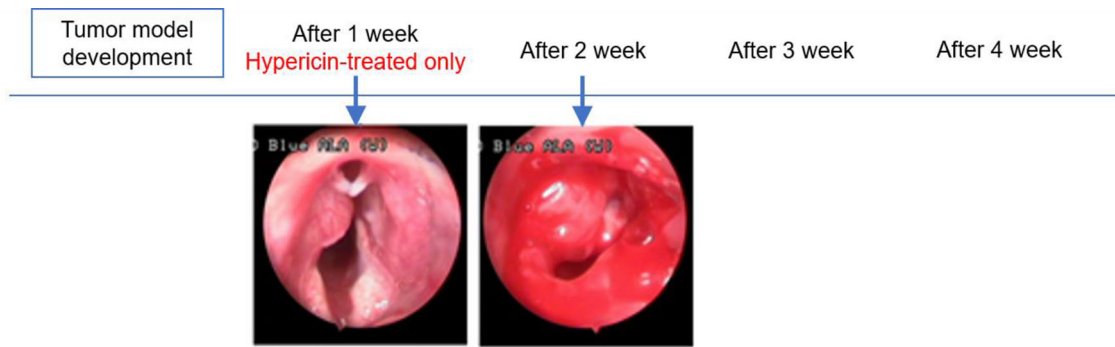
Fig. 11 In group C administered only hypericin, tumor growth occurred and all animals died 1 to 2 weeks following the procedure
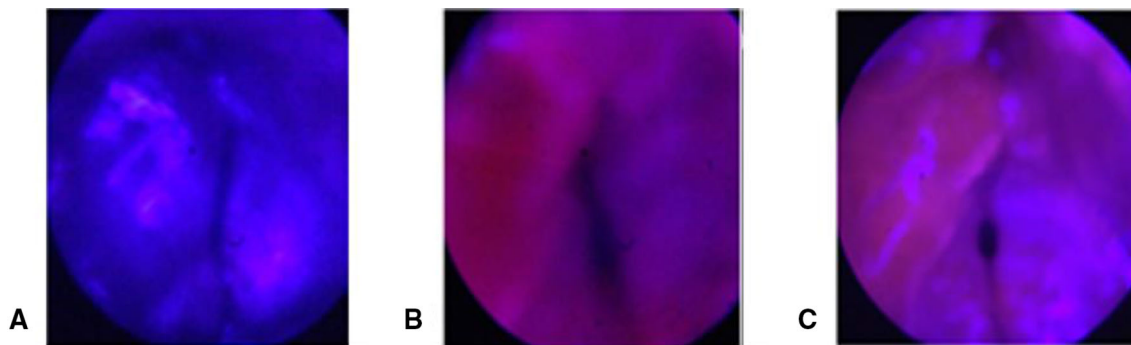

Fig. 12 Selective accumulation of HYP obtained after 1 week of **A** laser therapy only, **B** photodynamic therapy, and **C** hypericin-treated only, respectively
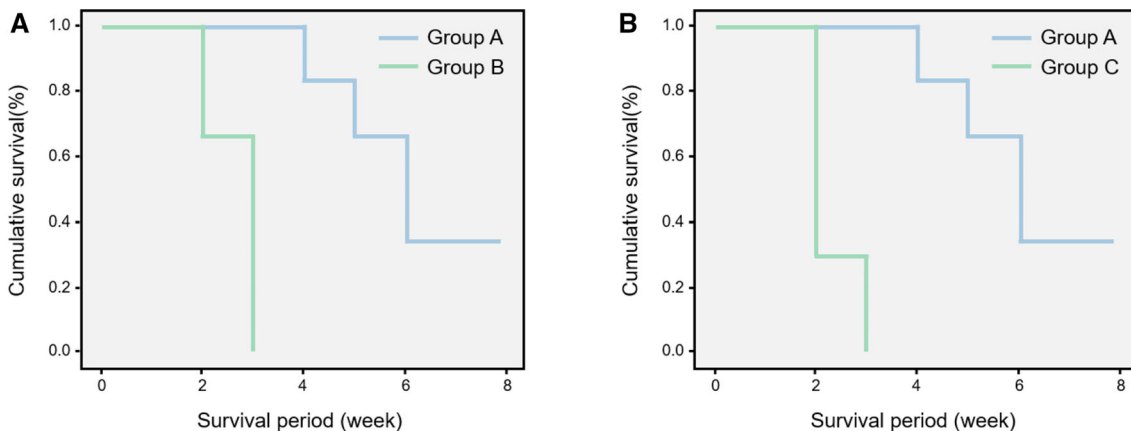

Fig. 13 **A**, **B** Survival curves comparing Groups A and B and Groups A and C. Group A survived two-fold longer than the other groups, demonstrating clinically cured status ($p = 0.03$, $p = 0.04$, respectively). There was no difference between Groups B and C with respect to death due to tumor progression, and were shorter than in Group A

by rigid laryngoscopy. However, since these results are the only clinical evidence available to date, confirmation with pathological examination may support the adoption of this model in additional studies.

We demonstrated that HYP was selectivity accumulated at high concentrations only in tumor tissues. In PDD using HYP, when illuminated with blue light with wavelength less than 400 nm, red-colored fluorescence indicated the presence of tumor tissue. The normal tissue around the tumor was observed to display fluorescence of the same color; however, the normal tissue appeared thinner than the tumor tissue. These observations indicated that HYP can accumulate in the normal tissue; however, it was apparently washed out relatively faster or accumulated more slowly in normal tissue than in the tumor owing to remarkably fewer feeding arteries and more effective venous drainage compared with the tumor tissue. Hence,

the tumor could be differentiated from the normal tissue as tumor tissue displayed a darker red color.

In addition to diagnosis, we confirmed that the targeting of the tumor or selective accumulation of HYP in tumor tissue produced more significant therapeutic effects under PDT. When the tumor tissue was irradiated with a laser of an appropriate wavelength after HYP administration, the tumor site as well as the contralateral normal mucosa of the vocal cord became edematous. This finding demonstrated that high concentrations of HYP accumulated in tumor tissue, and this HYP could be excited and emit energy for the induction of apoptosis in tumor cells. However, low concentrations of HYP in normal tissue may have resulted in only inflammatory reactions such as edema. In rabbits not treated with HYP and subjected to PDT, such reactions did not occur in normal or tumor tissues. In the absence of HYP, the energy from the photodynamic reaction cannot result in apoptosis. Although HYP has excellent selectivity and targeting ability that support its use as a photosensitizer, several limitations still need to be overcome using advanced medical engineering, such as: (1) shallow depths, narrow widths, or unequal energy transfer of during PDT might result in thermal injury to normal tissue, and (2) the requirement for an additional console for real-time intraoperative monitoring of the effectiveness of PDT. Laser probes must be developed for the effective transfer of energy required for PDT to be focused on the accumulated HYP in the tumor mass. In particular, diffuser-type laser probe tips, such as cylindrical, frontal light, or mounted type (on a balloon catheter) diffusers, must be modified to transport energy effectively into the tumor.

In the future, we expect that PDD would routinely be applied intraoperatively to identify the margins for surgical resection without leaving any remnant cancer tissue. It is necessary to perform more extensive preclinical studies similar to our experiments, including the specialized emission protocol and instruments for better control, and miniature devices for easy application. PDT could be utilized as one of the therapeutic options for recurrent malignant tumors, especially in vital organs, such as lung or brain, without producing functional deterioration. Furthermore, we expect that resection of large malignant intrathoracic masses encircling the aortic arch and arch vesselslike carotid and subclavian arteriescould be completed with PDT without the need for vascular replacement procedures requiring cardioplegia and total circulatory arrest, which are associated with a high risk of complications.

In conclusion, we found that HYP was an effective tumor imaging agent for defining tumor margins from normal tissue and in sterilizing post-resection margins intraoperatively. We expect HYP-PDT may spur the development of diagnostic imaging tools based on *In vitro*

experiments with VX tumor cells and *in vivo* experiments with the laryngeal cancer rabbit model. After additional studies, HYP-PDT may become the preferred modality for clinical diagnosis and minimally invasive treatment of cancer. In future, HYP-PDT may be used as a curative therapy with functional organ preservation during the early-stage laryngeal cancer and for inhibition of tumor progression and metastasis in advanced-stage cancers with/ without combining PDT with chemotherapy and radiotherapy.

Compliance with ethical standards

Conflict of interest The authors declare that they have no conflict of interest.

Ethical statement The animal studies were performed after receiving approval of the Institutional Animal Care and Use Committee (IACUS) at Kosin University College of Medicine (IACUC approval No. KMAP 15-07).

References

1. Nakayama M, Laccourreye O, Holsinger FC, Okamoto M, Hayakawa K. Functional organ preservation for laryngeal cancer: past, present and future. Jpn J Clin Oncol. 2012;42:155–60.
2. von Beckerath MP, Reizenstein JA, Berner AL, Nordqvist KW, Landström FJ, Löfgren AL, et al. Outcome of primary treatment of early laryngeal malignancies using photodynamic therapy. Acta Otolaryngol. 2014;134:852–8.
3. Choi JS, Oh SH, Kim YM, Lim JY. Hyaluronic acid/alginate hydrogel containing hepatocyte growth factor and promotion of vocal fold wound healing. Tissue Eng Regen Med. 2020;17:651–8.
4. Jung SY, Tran AN, Kim HY, Choi E, Lee SJ, Kim HS. Development of acellular respiratory mucosal matrix using porcine tracheal mucosa. Tissue Eng Regen Med. 2020;17:433–43.
5. Xin Z, Kim SW, Oak C, Kwon DY, Choi JH, Ko TY, et al. Investigation of the clinical potential of polarization-sensitive optical coherence tomography in a laryngeal tumor model. Tissue Eng Regen Med. 2021;18:81–7.
6. Oak C, Ahn YC, Nam SJ, Jung MH, Hwang SS, Chae YG, et al. Multimodal imaging using optical coherence tomography and endolaryngeal ultrasonography in a new rabbit VX2 laryngeal cancer model. Lasers Surg Med. 2015;47:704–10.
7. Mahmood U, Cerussi A, Dehdari R, Nguyen Q, Kelley T, Tromberg B, et al. Near-infrared imaging of the sinuses: preliminary evaluation of a new technology for diagnosing maxillary sinusitis. J Biomed Opt. 2010;15:036011.
8. Tao YC, Fried D. Near-infrared image-guided laser ablation of dental decay. J Biomed Opt. 2009;14:054045.
9. Cerussi AE, Mishra N, You J, Bhandarkar N, Wong B. Monte Carlo modeling of light propagation in the human head for applications in sinus imaging. J Biomed Opt. 2015;20:035004.
10. Castano AP, Demidova TN, Hamblin MR. Mechanisms in photodynamic therapy: part two-cellular signaling, cell metabolism

and modes of cell death. Photodiagnosis Photodyn Ther. 2005;2:1–23.

11. Thomas C, MacGill RS, Miller GC, Pardini RS. Photoactivation of hypericin generates singlet oxygen in mitochondria and inhibits succinoxidase. Photochem Photobiol. 1992;55:47–53.

12. Thomas C, Pardini RS. Oxygen dependence of hypericin-induced phototoxicity to EMT6 mouse mammary carcinoma cells. Photochem Photobiol. 1992;55:831–7.

13. Stupáková V, Varinská L, Mirossay A, Sarisský M, Mojzis J, Dankovcík R, et al. Photodynamic effect of hypericin in primary cultures of human umbilical endothelial cells and glioma cell lines. Phytother Res. 2009;23:827–32.

14. Seitz G, Krause R, Fuchs J, Heitmann H, Armeanu S, Ruck P, et al. In vitro photodynamic therapy in pediatric epithelial liver tumors promoted by hypericin. Oncol Rep. 2008;20:1277–82.

15. Li L, Huang T, Liu H, Zang J, Wang P, Jiang X. Purification, structural characterization and anti-UVB irradiation activity of an extracellular polysaccharide from Pantoea agglomerans. Int J Biol Macromol. 2019;137:1002–12.

16. Wessels JT, Busse AC, Rave-Fränk M, Zänker S, Hermann R, Grabbe E, et al. Photosensitizing and radiosensitizing effects of hypericin on human renal carcinoma cells in vitro. Photochem Photobiol. 2008;84:228–35.

17. Seitz G, Warmann SW, Armeanu S, Heitmann H, Ruck P, Hoffman RM, et al. In vitro photodynamic therapy of childhood rhabdomyosarcoma. Int J Oncol. 2007;30:615–20.

18. Berlanda J, Kiesslich T, Oberdanner CB, Obermair FJ, Krammer B, Plaetzer K. Characterization of apoptosis induced by photodynamic treatment with hypericin in A431 human epidermoid carcinoma cells. J Environ Pathol Toxicol Oncol. 2006;25:173–88.

19. Blank M, Lavie G, Mandel M, Hazan S, Orenstein A, Meruelo D, et al. Antimetastatic activity of the photodynamic agent hypericin in the dark. Int J Cancer. 2004;111:596–603.

20. Hanna NM, Waite W, Taylor K, Jung WG, Mukai D, Matheny E, et al. Feasibility of three-dimensional optical coherence tomography and optical Doppler tomography of malignancy in hamster cheek pouches. Photomed Laser Surg. 2006;24:402–9.

21. Yoneda T, Kitamura M, Ogawa T, Aya S, Sakuda M. Control of VX2 carcinoma cell growth in culture by calcium, calmodulin, and prostaglandins. Cancer Res. 1985;45:398–405.

22. Thibaut S, Bourré L, Hernot D, Rousset N, Lajat Y, Patrice T. Effects of BAPTA-AM, Forskolin, DSF and Z.VAD.fmk on PDT-induced apoptosis and m-THPC phototoxicity on B16 cells. Apoptosis. 2002;7:99–106.